A Compact Source–Load Agnostic Flexible Rectenna Topology for IoT Devices

Aline Eid, Jimmy G. D. Hester, Joseph Costantine, *Senior Member, IEEE*, Youssef Tawk, Ali H. Ramadan, and Manos M. Tentzeris, *Fellow, IEEE*

***Abstract*— This article presents a new compact lightweight radio frequency (RF) energy harvesting system. The system relies on a dual-tapered transmission line-based matching network that stretches the rectification capability of an integrated Schottky diode. This topology is demonstrated on a 2.4 GHz rigid harvesting system with a resulting power conversion efficiency that reaches up to 58% over 0 dBm input RF power. Its performance is compared with a reference rectifier that relies on a typical open circuit shunt-stub matching network. The rectifier along with a miniaturized monopole antenna is then tailored for a flexible substrate with a resulting efficiency around 50% at 0 dBm input power. The rectifier exhibits an almost flat efficiency over the 2.3–2.5 GHz frequency span despite wide load variations. The system is characterized in multiple bent configurations featuring high and stable performance. It is demonstrated that for different bent states, the proposed flexible harvester does not display large variations in harvested power. Thus, the presented rectenna demonstrates the remarkable combination of compactness, flexibility, and stability. Equipped with these features, such rectifier can be plugged into a variety of sensors, even on wearable surfaces, which makes it ideal for Internet of Things (IoT) applications.**

***Index Terms*— IEEE 80211 b/g, power conversion efficiency (PCE), radio frequency (RF) energy harvesting, rectenna, Wi-Fi, wireless power transfer.**

I. Introduction

THE projected number of deployed Internet of Things (IoT) devices is expected to reach billions in the upcoming years, which has an immediate implication on the number of batteries that need to be continuously charged and replaced. The design and realization of compact, energy autonomous, self-powered systems is therefore highly desirable. One potential way of satisfying these goals is through electromagnetic energy harvesting. This technique enables a new form of green technology that allows the "recycling" of ambient radio frequency (RF) energy. The RF energy harvesting system relies on an efficient and well-designed "rectenna," which is a combination of an antenna structure and an RF rectifying circuit. The antenna must be designed to collect the maximum RF energy in a certain environment. The captured RF signal is then transformed into a dc output through a rectifying circuit. Such dc output can then be fed into a compact IoT component [1].

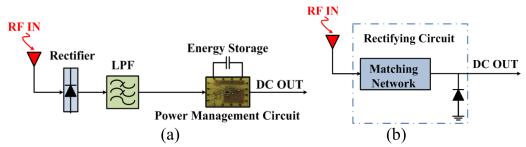

Fig. 1. RF energy harvester with single-stub matching network. (a) Block diagram of a basic RF energy harvesting system. (b) Block diagram of the considered rectifier schematic.

Rectifiers are classified by their ability to efficiently convert the RF signal into direct current (dc) with a minimum power dissipation along the way [2]–[6]. After the rectifying element, a low pass filter (LPF) is usually placed to ensure that only the dc component is delivered to the load. Finally, the recovered dc output is stored in a capacitor or a battery. A power management circuit is usually integrated to regulate and boost the output dc voltage. A block diagram of the basic RF energy harvesting system is shown in Fig. 1(a). Various rectenna systems have been presented in the literature, featuring characteristics such as flexibility, compactness, or wideband operation. In fact, the work presented in [7] resorts to novel 3-D printed structures using inkjet printing. In [8], two different types of energy harvesting systems are presented, based on additive manufacturing techniques (AMTs) that utilize ambient energy to power up connected wireless modules. AMTs are capable of producing conformal devices by relying on flexible substrates. Printing on flexible material is also accompanied by depositing any type of conducting or dielectric material on a bendable nonplanar surface or component. An example is shown in [9] where a multiband RF energy harvester is fabricated on a paper substrate. The proposed rectifier in [9] presents an efficiency in the range of 11%–30% at −15 dBm input power over LTE bands.

The work presented in this article, primarily focuses on enhancing the ability of standard shunt Schottky diode topologies used for energy harvesting in rectenna systems. Such enhancement is achieved by simultaneously enabling flat and high-power conversion efficiencies across an entire frequency band of interest. Such expansion in the harvesting

Manuscript received July 3, 2019; revised October 5, 2019; accepted November 15, 2019. Date of publication November 28, 2019; date of current version April 7, 2020. This work was supported by the American University of Beirut Research Board. *(Corresponding author: Joseph Costantine.)*

A. Eid is with the Electrical and Computer Engineering Department, American University of Beirut, Beirut 1107 2020, Lebanon, and also with the School of Electrical and Computer Engineering, Georgia Institute of Technology, Atlanta, GA 30309 USA (e-mail: aeid7@gatech.edu).

J. G. D. Hester is with the School of Electrical and Computer Engineering, Georgia Institute of Technology, Atlanta, GA, 30309 USA, and also with Atheraxon, Atlanta, GA 30340 USA (e-mail: jimmy.hester@gatech.edu).

J. Costantine and Y. Tawk are with the Electrical and Computer Engineering Department, American University of Beirut, Beirut 1107 2020, Lebanon (e-mail: jcostantine@ieee.org; yatawk@ieee.org).

A. H. Ramadan is with the Electrical Engineering Department, Fahad Bin Sultan University, Tabuk 71454, Saudi Arabia (e-mail: ramadan@ieee.org).

M. M. Tentzeris is with the School of Electrical and Computer Engineering, Georgia Institute of Technology, Atlanta, GA 30309 USA (e-mail: etentze@ece.gatech.edu).

Color versions of one or more of the figures in this article are available online at http://ieeexplore.ieee.org.

Digital Object Identifier 10.1109/TAP.2019.2955211

capability is dependent on several factors that start by improving the matching between the antenna and the input of the Schottky diode. Flattening the efficiency response of the rectenna system as a function of load variations can be achieved by resorting to tapering techniques [10]–[12]. However, the range over which the efficiency flatness has been achieved is narrow [10]–[12]. In this article, common challenges faced in wireless sensors and IoT nodes are addressed by proposing energy powering solutions exhibiting robustness, flexibility, and load tolerance. Wireless nodes require rapid deployment, autonomous operation, and flexibility accompanied with low cost and fault tolerance characteristics. The aim of this work is to provide a solution that meets the aforementioned requirements through the design of a compact, very lightweight, and low cost flexible RF energy harvester. The authors propose in this article, a novel rectenna system that provides a stable efficiency response across a large variation of load (from 0.1 to 7 kΩ), frequency operation (2.3–2.48 GHz), and input power fluctuations (−20 to 3 dBm). With this property, the proposed rectenna is suitable for integration into IoT devices, sensors, or nodes with minimum required fitting. The new rectenna topology relies on a new and improved matching network that resorts to tapered and balanced microstrip lines to improve and stabilize its performance. In addition, the originality of the work presented in this article is based on pushing the limits of the Schottky diode's rectification abilities by optimizing the matching network's topology. Another novelty aspect relies on the miniaturization aspect of the overall rectifier circuit without sacrificing the stability and efficiency of the rectenna. Additional novelty resides in the implementation of a compact lightweight rectenna on a flexible substrate that is characterized in multiple bent configurations. Such flexible rectenna features high and stable performance with less than 57% variation in harvested power. The work presented herein is, to the best of our knowledge, the first of a kind, rectenna system that is stable across large load deviations. Hence, it can be considered universally adaptable for a plethora of sensor implementations.

Section II presents the design of the new and improved matching network and its integration in rectifiers based on rigid substrates. Section III presents a performance analysis of the proposed matching networks with regard to load, frequency, and input power variations. Section IV presents the implementation of the rectifier on a flexible substrate in a compact rectenna system. The flexible rectenna is then tested over different curvatures, thereby demonstrating its ruggedness. This section also includes a table of comparison with previously reported work demonstrating the rectifier's remarkably high conversion efficiency relative to its electrical size. Section V concludes this article.

II. New Dual Line Tapered Matching Technique

The work presented in this article focuses on harvesting RF energy in the ISM 2.4 GHz frequency band. This work relies solely on Schottky diodes, and in particular, the SMS7630 zero-bias, from Skyworks [13]. This diode is employed due to its low built-in potential that is about 170 mV for ∼1 mA forward current. Such diode is also

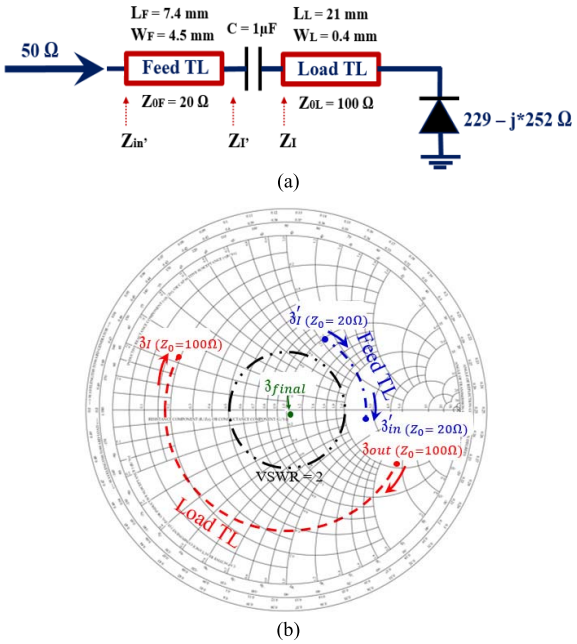

Fig. 2. (a) Proposed dual-line matching network. (b) Smith chart representation of the proposed impedance transformer matching network.

suitable for applications that operate at relatively low input power levels. In particular, the rectenna system proposed herein relies on a shunt connected Schottky diode as shown in Fig. 1(b). It is mainly composed of a receiving antenna and an impedance matching network followed by a single Schottky diode. The focus is to improve the matching conditions between the antenna and the rectifying element in order to minimize the losses across the full designed network. Thus, the power conversion efficiency (PCE), given by the following equation, constitutes the main parameter for the system's evaluation:

$$PCE = \frac{P_{DC}}{P_{RF}} * 100 = \frac{V_{DC}^2}{R_L * P_{RF}} * 100(\%) \tag{1}$$

where P_{DC} represents the dc power collected at the output, P_{RF} is the RF power captured by the antenna, V_{DC} denotes the dc voltage at the output, and R_L is the load impedance.

The rectifier circuit presented in this article is designed to allow the PCE to maintain an almost flat response for a wide range of load and input power variations. Such behavior is obtained by proposing a new dual line-based matching network along with the integration of the appropriate tapered sections. The layout of the presented matching network is depicted in Fig. 2. It consists of two transmission lines (i.e., load TL and feed TL) that have different characteristic impedances and electrical lengths. The TL, characterized by an impedance (Z_{0L}), a phase constant (β_L), a length (L_L), and a width (W_L), constitutes the "load TL." The purpose of the load TL is to transform the diode's impedance (Z_{out}) into (Z_I). The second TL in series is the "feed TL" that is characterized by an impedance (Z_{0F}), a phase constant (β_F), a length (L_F), and a width (W_F). A capacitor (C) prevents the dc voltage generated by the diode from reaching the generator.

The lengths of both TLs are iteratively swept and optimized over a full spatial period (0–0.5$*\lambda_g$). The maximum value

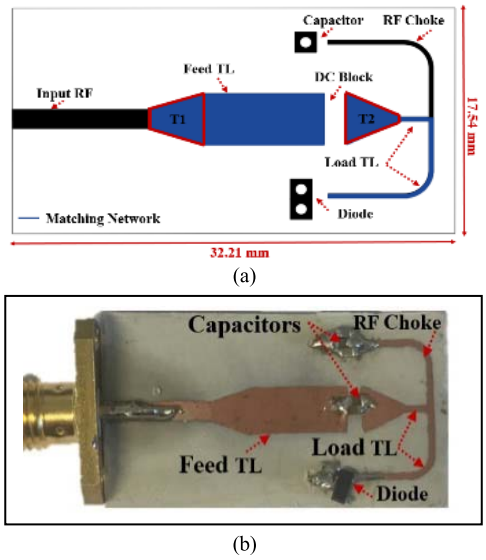

Fig. 3. (a) Layout of the rectifier with a balanced matching network. (b) Fabricated rectifier prototype.

chosen for either (Z_{0L}) or (Z_{0F}) is 100 Ω to take into consideration practical fabrication tolerances whereas the minimum impedance value is 20 Ω to keep the overall design as compact as possible with a minimum amount of losses. The change in the impedance at various points along the proposed matching network is demonstrated on the Smith chart in Fig. 2(b). The diode is located on the "Load TL" that has $Z_{0L} = 100$ Ω. Therefore, its impedance ($229 - j252$ Ω at 2.45 GHz and for an input power level of −10 dBm) is first normalized to 100 Ω and placed on the smith chart as ($\mathfrak{Z}_{out}$). The $\lambda_g/4$ "Load TL" line transposes the diode impedance from ($\mathfrak{Z}_{out}$) to ($\mathfrak{Z}_I$) as shown in Fig. 2(b). At this stage, the impedance faces the "feed TL" that has $Z_{0L} = 20$ Ω. The transformation from 100 to 20 Ω is done by first denormalizing ($\mathfrak{Z}_I$) to 100 Ω and then normalizing it back to 20 Ω. This corresponds to the point ($\mathfrak{Z}'_I$) on the smith chart of Fig. 2(b). This point is then moved by a distance of $0.0986\lambda_g$ to reach the point ($\mathfrak{Z}'_{in}$). Such distance is equivalent to the length of the "feed TL." Denormalizing this point to 20 Ω leads to the input impedance of the circuit being equal to $(52 - j4)$ Ω. The resulting impedance is now normalized to 50 Ω, which results in the point $(\mathfrak{Z}_{final}) = 1.04 - j0.08$ as indicated on the smith chart inside the VSWR = 2 circle.

The proposed matching network is then integrated within the full rectifier circuit along with the Schottky diode and the required RF chokes. The rectifier is designed and simulated using Keysight Advanced Design System (ADS) [14], while employing large signal S-parameters (LSSP) and harmonic balance (HB) simulations. The rectifier is initially terminated by a load of 1 kΩ and the design is based on Rogers 3203 ($h = 0.508$ mm and $\varepsilon_r = 3.02$). The corresponding topology is shown in Fig. 3(a). The rectifier layout includes two triangular tapered sections T1 and T2 in order to ensure a smooth transition between the various TLs of the matching network [15]. The objective of T1 is to transition from the 50 Ω feeding line to the characteristic impedance of "feed TL" that is found to be 20 Ω. As for T2, its function is to enable the transition from 20 Ω to the characteristic impedance of "load TL" that is 100 Ω.

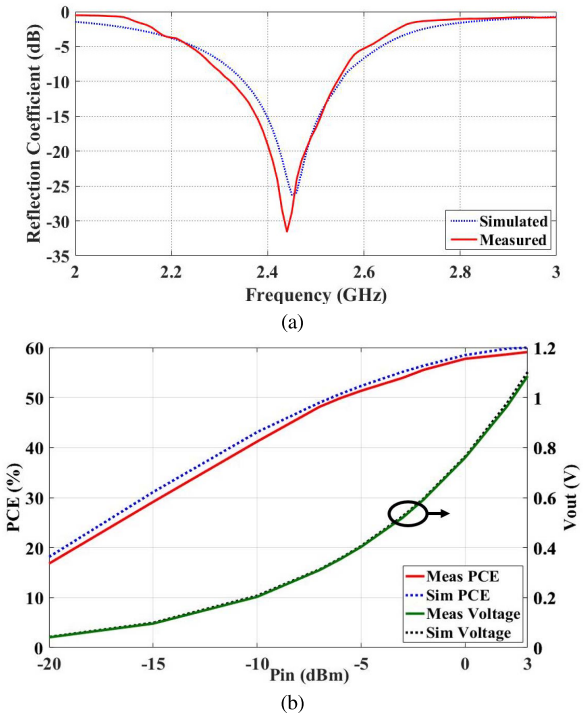

Fig. 4. Comparison between simulated and measured results for (a) reflection coefficient for the rectifier and (b) PCE and output voltage for a load of 1 kΩ.

These tapered sections play a fundamental role in achieving a stable PCE response over a wide range of load variations. The RF choke functionality is achieved using a shorted quarter-wavelength ($\lambda_g/4$) stub that is terminated by 1 μF capacitor. This stub is specifically designed to behave as an open circuit impedance at the fundamental and third harmonic frequencies while presenting a short circuit to the second harmonics.

The position of the "load TL" is tuned with respect to the Schottky diode resulting in a balanced topology. Namely, part of the "load TL" is kept in series with the "feed TL" whereas the other part is suspended in shunt with the Schottky diode at its end.

The rectifier circuit is fabricated as shown in Fig. 3(b). For both simulated and measured results, the presented rectifier is matched for operation within the entire desired frequency range as summarized in Fig. 4(a). The fabricated prototype exhibits a total compact size of 32.21 mm × 17.54 mm. By inspecting the voltage and efficiency results in Fig. 4(b), an efficiency of 58% is observed at 0 dBm with a peak voltage of 0.76 V measured for a 1 kΩ load. For these two results, a close agreement is noticed between simulated and measured data.

III. Performance Analysis With Respect to Frequency, Load, and Input Power

The performance of the proposed matching network herein is evaluated for a variation of load impedances. Such analysis is essential to meet the objective of this work, which is based on proposing a universal rectifier circuit whose performance is load agnostic. The input impedance of the integrated Schottky diode varies, not only with frequency, but also with the RF power fed to the rectifier. Hence, a comparative analysis is exe-

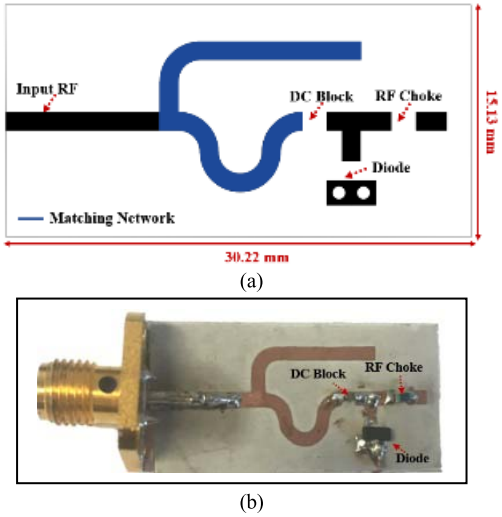

Fig. 5. (a) Layout of the reference rectifier circuit that relies on open-circuit shunt stub. (b) Fabricated prototype.

cuted in this section to analyze the performance of the rectifier with respect to frequency, load, and input power variations. The performance of the presented rectifier is compared with a reference rectifier that adopts a typical matching technique based on open-circuit shunt stub. The purpose of that comparison is to highlight the superior performance of the designed rectifier with respect to traditionally proposed circuits.

The reference rectifier circuit along with its fabricated prototype is presented in Fig. 5. Such rectifier is matched using an open-circuit stub that has a length of $L_{OC\_stub} = 0.198\lambda_g$ (15.8 mm). A distance $d_{OC\_stub} = 0.16\lambda_g$ (12.8 mm) away from the load is adopted as shown in Fig. 5. Miniaturization by relying on a meandering technique is applied to the two lines to keep the resulting rectifier compact in size and similar in area to the proposed rectifier shown in Fig. 3. As a result, the reference rectifier's dimensions are 30.22 mm × 15.13 mm, thus achieving a 51% reduction in size in comparison to a nonmeandered stub. A 1 μF dc-blocking capacitor and a 110 nH RF choke are integrated within the matching network. This rectifier is matched over the entire desired band and exhibits a good efficiency of 51.26% at 0 dBm with a peak measured voltage of 0.716 V and an optimal load of 1 kΩ.

A. Effect of Load Variation

The PCE behavior of the proposed and the reference rectifier circuits with respect to load variations for an RF fed power of 0 dBm at 2.45 GHz is shown in Fig. 6(a). For both circuits, the efficiency peaks at the optimal load value of 1 kΩ. The proposed tapered topology exhibits a larger difference in comparison to the open-circuit shunt stub matching network.

The PCE of the proposed rectifier in this article peaks at 58% as shown in Fig. 6(a) and is able to maintain 29% (i.e., almost 50% of the peak) between 0.1 and 7 kΩ. On the other hand, the PCE of the open stub rectifier peaks at 51% and maintains 50% of its peak efficiency (i.e., 25.5%) between 0.1 and 5 kΩ. Hence, it is clear that the proposed rectifier is more immune to load-variations than a conventional one.

Furthermore, the input impedance of the proposed rectifier exhibits a much higher stability across a large variation of load

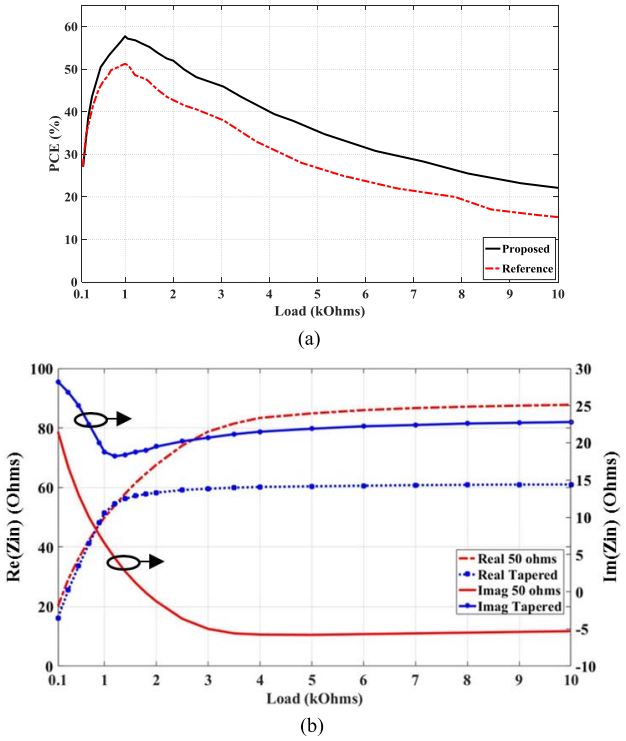

Fig. 6. Measured PCE results for different load values of both the proposed and reference rectifiers at $Pin = 0$ dBm and $f = 2.45$ GHz. (b) Input impedance plots with respect to load variations for the proposed and reference rectifiers.

as shown clearly in Fig. 6(b). It is noticed that the real part of the input impedance reaches a value around 50 Ω for a load of 1 kΩ corresponding to the peak efficiency result. Both the real and imaginary parts then maintain a steady-state response across the remaining load variations.

However, the input impedance of a 50 Ω-line-based conventional rectifier reaches a value of 50 Ω for a load of 1 kΩ, corresponding to its peak efficiency. However, both the real and imaginary part deviate away from stabilizing till a load of between 4 and 5 kΩ, while exhibiting much larger variations in the impedance as whole. It is also important to note that for such a conventional rectifier, the real part of its input impedance deviates largely from 50 Ω for most of the load range.

Specifically, the real part of the input impedance of the proposed rectifier with tapered sections increases from 16 to 58 Ω when the load goes from 0.1 to 2 kΩ. Then, it is stabilized along all the remaining load ranges.

A similar performance is achieved by the imaginary part of the input impedance where it decreases from j28 to j19 Ω before stabilizing for the remaining load ranges. However, the real part of the reference rectifier increases from 20 to 88 Ω throughout the range, while the imaginary part decreases from j21.5 Ω to a stable state of around −j5 Ω. This behavior explains the ability of the proposed rectifier in maintaining a better power transfer capability with respect to load variations as clearly validated by Fig. 6(b). Therefore, the tapering technique implemented between the lines of different characteristic impedances allows the circuit to maintain better efficiency figures over a wider drift of load values.

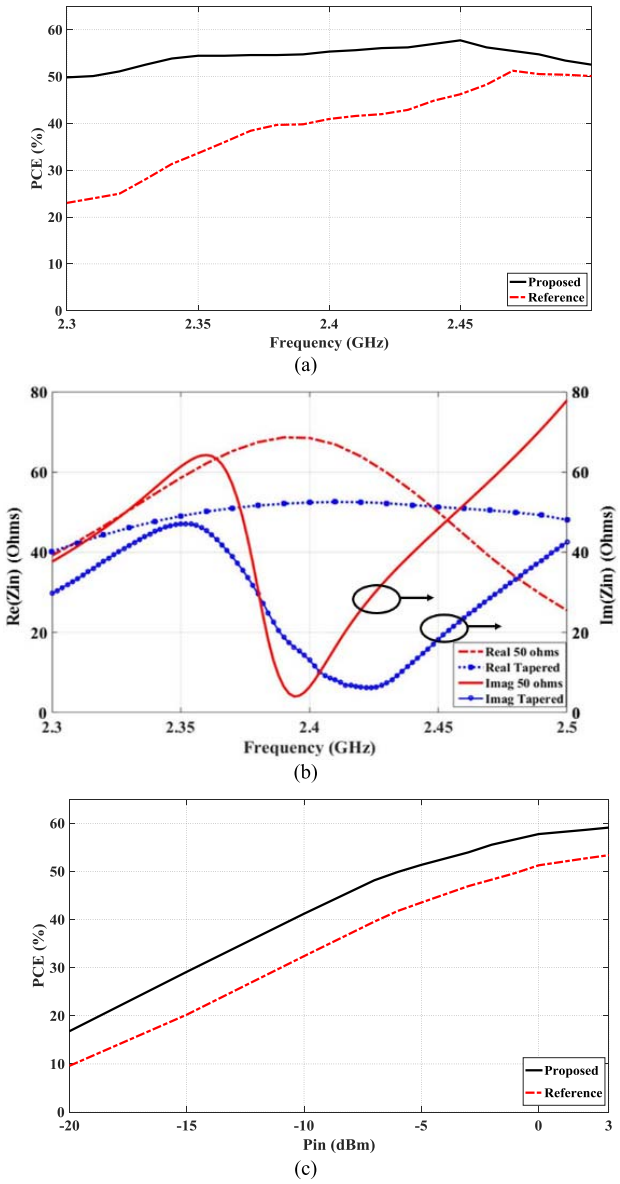

Fig. 7. Measured PCE results for a span of frequencies. (b) Input impedance plots with respect to frequency for the proposed and reference rectifiers. (c) Measured PCE when varying the input fed power.

B. Effect of Frequency Variation

The PCE performance is also studied when the frequency is varied between 2.3 and 2.5 GHz as shown in Fig. 7(a). Such study is done for an input power of 0 dBm and for the corresponding optimal load of 1 kΩ. The proposed rectifier maintains an almost stable efficiency around 55% over the entire frequency range. This is due to its tapered matching network.

The reference rectifier shows more dependence with respect to the variation of frequency. It is noticed that the efficiency flatness for the reference rectifier appears in a very small fraction of the frequency band. This behavior is explained by the use of solely 50 Ω TLs, which offer a narrower bandwidth in comparison with tapered lines. The tapered lines' circuit displays smoothness in the input impedance with respect to the variation in frequency. More specifically, the real part of the proposed rectifier circuit starts at 42 Ω, increases until it reaches 50 Ω and then returns to 46 Ω while the imaginary part smoothly changes as the frequency increases. The input impedance variation with respect to frequency is shown in Fig. 7(b).

On the other hand, the reference rectifier for example reacts differently to the changes in frequency. Its input impedance variation shows abrupt increases and decreases within a smaller frequency range.

C. Effect of Input Power Variation

The performance of the proposed rectifier is also affected by the variation in the input RF power levels. Fig. 7(c) illustrates the measured PCE values for a load of 1 kΩ and an optimal frequency of operation (2.45 GHz) with respect to a range of input power spanning from −20 to 3 dBm.

Similar to previous analysis, the proposed rectifier circuit presents the highest efficiency over the entire span of the input power. Such analysis proves the superior performance of the proposed rectifier circuit with a tapered matching network and nonuniform characteristic impedances. Such behavior that exhibits great stability along with independence of environment and type of connected load, enables this rectifier to be considered as a successful plug-in for a large variety of sensors within a diversity of applications. With flexibility added to it, the proposed rectifier along with its corresponding antenna can also be integrated on nonplanar or even wearable surfaces. Such behavior makes it ideal for IoT device integration.

IV. Flexible Compact Rectenna Design

In order to verify its suitable performance over a flexible surface, the proposed rectifier is now fabricated on a 0.18 mm-thick liquid crystal polymer (LCP) substrate (dielectric constant of 3). The fabrication is based on using an inkjet-printed masking technique followed by etching [16]. The layout of flexible design is shown in Fig. 8(a), which displays slight variation from its rigid counterpart of Fig. 3(a) in terms of line widths and dimensions.

The measured and simulated PCE results are shown in Fig. 8(b). This rectifier achieves an efficiency of above 40% at 2.4 GHz around the 0 dBm input power and $R_L = 1$ kΩ load operation point. It is also important to note that the flexible rectifier reaches a peak efficiency of 50% at 2.37 GHz.

The rectifier's performance is also evaluated in function of load and frequency variations to demonstrate the robustness of the proposed matching technique in preserving a stable response on flexible substrates. Fig. 8(c) shows the rectifier's measured PCE when the load is varied from 0.1 to 10 kΩ while Fig. 8(d) presents the case when the frequency is swept from 2.3 to 2.48 GHz, respectively. The corresponding results for the proposed rectifier on rigid RO3203 substrate are also embedded in these two figures [Fig. 8(c) and (d)]. The rectifier exhibits a very similar robust behavior on both rigid and flexible substrates with respect to load and frequency variations. The flexible rectifier's efficiency preserves a value above 36% over a wide range of frequencies while showing a robust performance in function of abrupt load variations. The flexible rectifier circuit is then integrated into a rectenna configuration by cascading it with a compact flexible monopole antenna. A schematic illustration of the monopole antenna design along

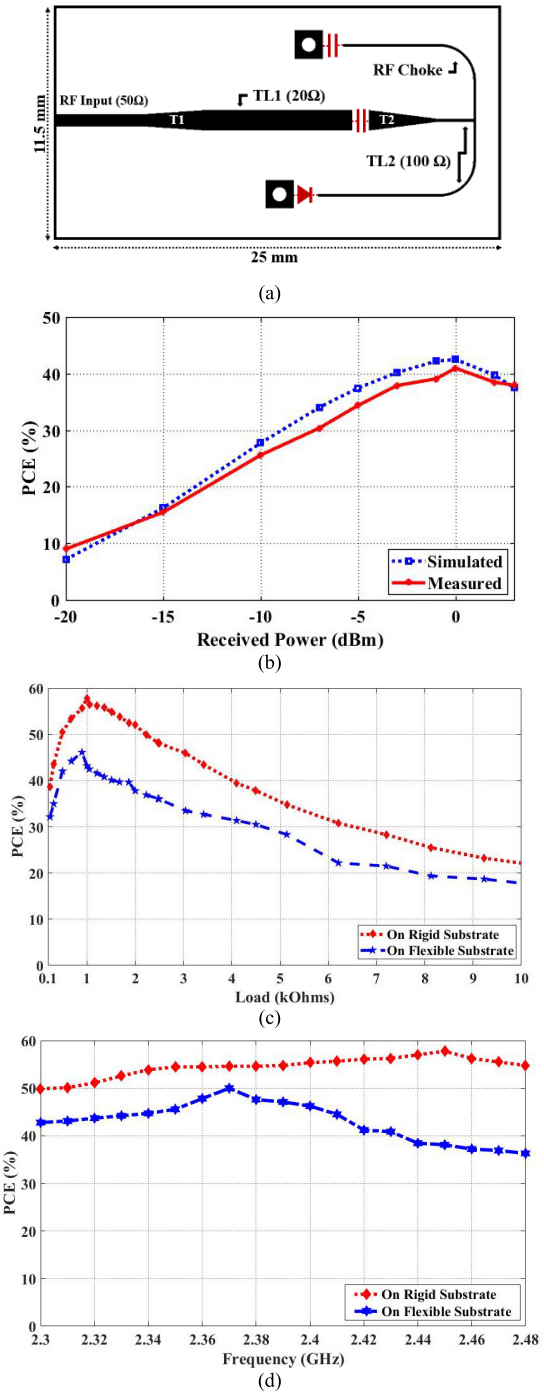

Fig. 8. (a) Layout of the flexible rectifier. (b) Simulated and measured PCE for the rectifier design based on the flexible substrate. Measured PCE for both the flexible and rigid designs (c) as a function of load variations and (d) as a function of a given span of frequencies.

with its dimensions are shown in Fig. 9(a). This design involves a meandered shape monopole in order to miniaturize its size and allow its operation at 2.4 GHz. The design is fabricated on LCP substrate with a thickness of 0.18 mm and a size of 15.1 mm × 8.15 mm. The meandered monopole antenna exhibits a gain of 0 dBi with a reflection coefficient S_{11} that is below −10 dB within the frequency range of interest as shown in Fig. 9(b) and (c). It is important to highlight the fact that the flexible rectenna still exhibits flatness and robust performance regardless of the curvature radius, load variations,

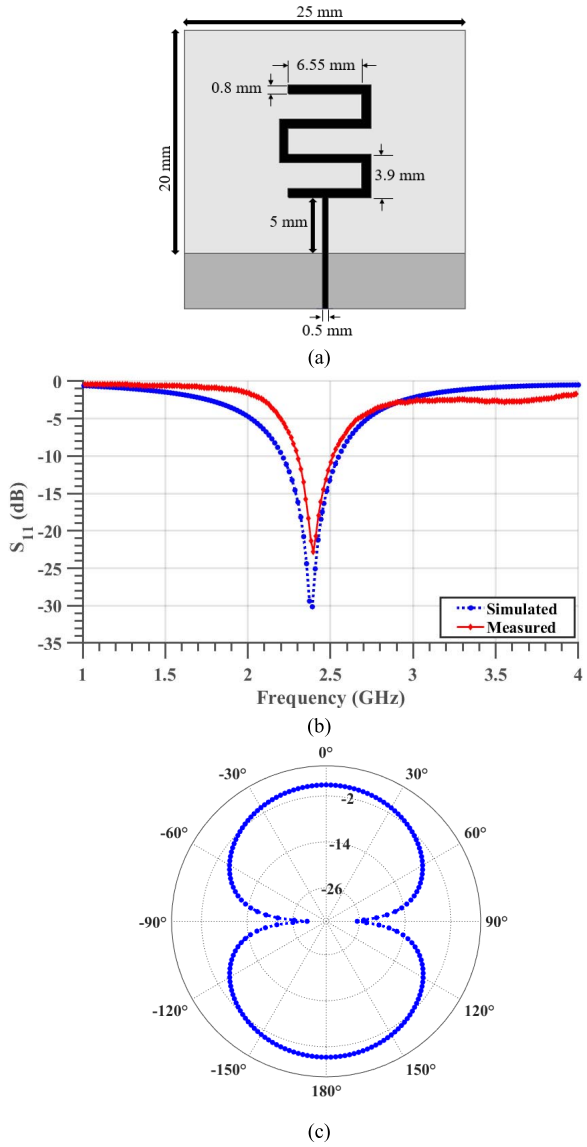

Fig. 9. Flexible monopole antenna. (a) Schematic of the 2.4 GHz meandered monopole. (b) Simulated and measured reflection coefficient of the designed monopole antenna. (c) Plot of the simulated gain of the antenna (f = 2.4 GHz and $\varphi = 90°$).

input power, or frequency operation. Such performance is exemplary especially for nonplanar surface integration.

The antenna and rectifier, integrated into one circuit, form a rectenna with an overall size of 50 mm × 11.5 mm as shown in Fig. 10(a). It is proven that the resulting rectenna offers compactness as well as flexibility and ease of integration. For validation purposes, its performance is tested over curvatures of different bending radii. The rectenna system is characterized as a function of its received power density. The system is illuminated from a distance of 65 cm with a horn antenna, whose gain is 5.85 dBi and RF input power is swept from 10 to 30 dBm. Using Friis transmission equation [17], the received RF power at the input terminals of the rectifying circuit is then determined to be varying between −20 and 0 dBm. The rectifier is loaded with its 1 kΩ optimal load impedance and the output dc power of the rectenna system is measured for four bending scenarios over a range of incident power densities at the receiving antenna.

TABLE I
PERFORMANCE COMPARISON

Ref.	Freq. (GHz)	Diode Type & Topology	P_{In} (dBm)	Substrate	Rectifier Active Area (mm^2)	PCE (%)	BW within 10% of peak PCE (MHz)	FOM
[18]	2.412	HSMS2850 Shunt	0	NPC-F260 $\varepsilon_r = 2.6$ h = 0.8 mm	32 x 32	53	60	3.07
[19]	2.450	SMS7630 Series	0	Arlon 25N $\varepsilon_r = 3.38$ h = 0.76 mm	19 x 21	39	100	4.34
[20]	2.450	SMS7630 Voltage Doubler	0	RT/5880 $\varepsilon_r = 2.2$ h = 1.57 mm	38 x 24	48	NA	3.58
[21]	2.450	SMS7630 Voltage Doubler	0	FR4 $\varepsilon_r = 4.4$ h = NR	37 x 5.5	35	NA	5.85
[22]	1.85	SMS7630 Series	0	PET $\varepsilon_r = 3.3$ h = 0.075 mm	60 x 55	35	75	0.85
[9]	1.8	HSMS2850 Series	0	Paper $\varepsilon_r = 2.55$ h = 0.23 mm	35 x 30	40	100	4.14
[This work] Rigid Substrate	2.450	SMS7630 Shunt	0	Rogers 3203 $\varepsilon_r = 3.02$ h = 0.508 mm	24.21 x 17	58	180	7.01
[This work] Flexible Substrate	2.45	SMS7630 Shunt	0	LCP $\varepsilon_r = 3$ h = 0.18 mm	17 x 10	40	140	11.73

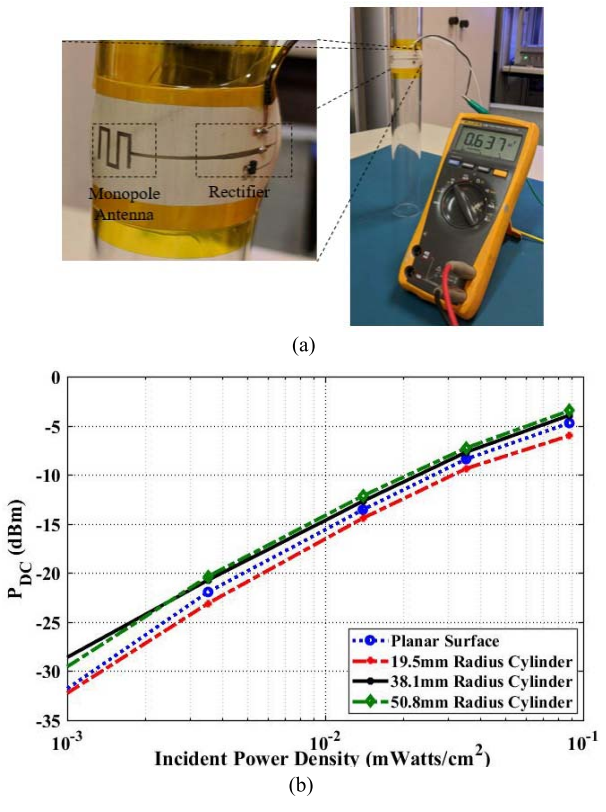

Fig. 10. Flexible rectenna fabrication and measurement. (a) Flexible 2.4 GHz rectenna measured on the 19.05 mm radius cylinder. (b) Measured dc output power for different cylinders' radii.

The rectenna maintains a stable performance for several configurations over planar or curved surfaces as shown in Fig. 10(b). The curved surface employed for testing is cylindrically shaped with curvatures of 19.05, 38.1, and 50.8 mm radii. It is important to note that the dc power variation is low even at its maximum value when bending occurs. Such variation is estimated to be less than 57%, which is considered superior in comparison to traditional flexible rectenna structures. The rectenna efficiencies are extracted and calculated from the dc output power measurements for both bent and planar scenarios. As expected from Fig. 10(b), where the rectenna's output dc power is very stable with minimal variations under planar and bent conditions, the calculated efficiencies maintain a very similar behavior to the one shown in Fig. 8(b). The range goes from approximately 5%–10% to 35%–42% for a received power at the input of the rectenna of −20 to 0 dBm. This stability demonstrates the remarkable adequacy of this circuit for bent implementations.

The compactness and efficiency of the proposed rigid and flexible rectifiers are finally benchmarked using the figure of merit (FOM) shown in (2). The FOM, shown in (2), takes into account the rectifier PCE per unit of electrical area (area normalized to the effective wavelength at the operating frequency of the harvester)

$$FOM = \frac{PCE}{100 * A_{Normalized}} \quad (2)$$
$$\text{with } A_{Normalized} = \frac{Area_{Rectifier}}{\lambda^2} \text{ and } \lambda = \frac{c}{\sqrt{\varepsilon_r} * f}$$

where the PCE denotes the power conversion efficiency of the rectifier, the $A_{Normalized}$ takes into account the active area of the rectifier normalized to the square of the wavelength, λ is the wavelength,c is the speed of light, ε_r is the relative permittivity, and f is the frequency of operation.

The FOM of the two rectifiers built on rigid and flexible substrates are calculated and included in Table I for comparison with several state-of-the-art work as presented in [9] and [18]–[22]. Table I highlights the outperformance of the proposed technique and design in both rigid and flexible architectures. Such performance is highlighted by maintaining both high and flat efficiency values despite the miniaturization aspect of the whole system.

V. Conclusion

In this article, a compact rectenna topology is proposed and implemented. The rectifier component is first introduced on rigid and flexible substrates with a new matching network that allows a stable efficiency response across a variation of loads, frequency, and power ranges. The proposed matching network resorts to two series lines of nonuniform characteristic impedances. The effect of adding tapered sections is proven to improve the overall performance stability of the rectifier circuit. The performance of the proposed rectifier is compared with a standard rectifier that relies on single shunt stub matching network. A flexible 2.4 GHz compact rectenna system is also presented and tested. It displays an unprecedented combination of properties with compactness, high efficiency, flexibility and stability relative to bending, load, and frequency variations. The presented work enables the advent of integrated flexible and reliable energy harvesting systems for IoT applications and introduces the concept of "universal" rectenna systems.

References

[1] W. Lin, R. W. Ziolkowski, and J. Huang, "Electrically small, low-profile, highly efficient, Huygens dipole rectennas for wirelessly powering Internet-of-Things devices," *IEEE Trans. Antennas Propag.*, vol. 67, no. 6, pp. 3670–3679, Jun. 2019.

[2] J. O. McSpadden, L. Fan, and K. Chang, "Design and experiments of a high-conversion-efficiency 5.8-GHz rectenna," *IEEE Trans. Microw. Theory Techn.*, vol. 46, no. 12, pp. 2053–2060, Dec. 1998.

[3] Y.-J. Ren and K. Chang, "5.8-GHz circularly polarized dual-diode rectenna and rectenna array for microwave power transmission," *IEEE Trans. Microw. Theory Techn.*, vol. 54, no. 4, pp. 1495–1502, Jun. 2006.

[4] Y.-H. Suh and K. Chang, "A high-efficiency dual-frequency rectenna for 2.45- and 5.8-GHz wireless power transmission," *IEEE Trans. Microw. Theory Techn.*, vol. 50, no. 7, pp. 1784–1789, Jul. 2002.

[5] T. S. Almoneef, F. Erkmen, and O. M. Ramahi, "Harvesting the energy of multi-polarized electromagnetic waves," *Sci. Rep.*, vol. 7, no. 1, Nov. 2017, Art. no. 14656.

[6] M. Roberg, T. Reveyrand, I. Ramos, E. A. Falkenstein, and Z. Popovic, "High-efficiency harmonically terminated diode and transistor rectifiers," *IEEE Trans. Microw. Theory Techn.*, vol. 60, no. 12, pp. 4043–4052, Dec. 2012.

[7] S. Kim *et al.*, "Ambient RF energy-harvesting technologies for self-sustainable standalone wireless sensor platforms," *Proc. IEEE*, vol. 102, no. 11, pp. 1649–1666, Nov. 2014.

[8] S. A. Nauroze *et al.*, "Additive manufacturing technologies for near-and far-field energy harvesting applications," in *Proc. IEEE Radio Wireless Symp. (RWS)*, Jun. 2016, pp. 159–161.

[9] V. Palazzi *et al.*, "A novel ultra-lightweight multiband rectenna on paper for RF energy harvesting in the next generation LTE bands," *IEEE Trans. Microw. Theory Techn.*, vol. 66, no. 1, pp. 366–379, Jan. 2018.

[10] A. Eid *et al.*, "An efficient RF energy harvesting system," in *Proc. Eur. Conf. Antennas Propag.*, Mar. 2017, pp. 896–899.

[11] A. Eid, J. Costantine, Y. Tawk, M. Abdallah, A. H. Ramadan, and C. G. Christodoulou, "Multi-port RF energy harvester with a tapered matching network," in *Proc. IEEE Int. Symp. Antennas Propag.*, Jul. 2017, pp. 1611–1612.

[12] J. Costantine, A. Eid, M. Abdallah, Y. Tawk, and A. H. Ramadan, "A load independent tapered RF harvester," *IEEE Microw. Compon. Lett.*, vol. 27, no. 10, pp. 933–935, Oct. 2017.

[13] Skyworks Solutions. (Jul. 5, 2016). *Surface Mount Mixer and Detector Schottky Diodes*. Accessed: Sep. 15, 2016. [Online]. Available: http://www.skyworksinc.com//uploads/documents/Surface_Mount_Schottky_Diodes_200041AB.pdf

[14] *Advanced Design System*, Keysight Technol., Santa Rosa, CA, USA, 2009.

[15] D. M. Pozar, *Microwave Engineering*, 4th ed. Hoboken, NJ, USA: Wiley, 2012.

[16] A. Eid *et al.*, "A flexible compact rectenna for 2.40 Hz ISM energy harvesting applications," in *Proc. IEEE Int. Symp. Antennas Propag. USNC/URSI Nat. Radio Sci. Meeting*, Jul. 2018, pp. 1887–1888.

[17] C. A. Balanis, *Antenna Theory: Analysis and Design*. Hoboken, NJ, USA: Wiley, 2016.

[18] Y. Huang, N. Shinohara, and H. Toromura, "A wideband rectenna for 2.4 GHz-band RF energy harvesting," in *Proc. IEEE WPTC*, May 2016, pp. 1–3.

[19] K. Niotaki, S. Kim, S. Jeong, A. Collado, A. Georgiadis, and M. M. Tentz, "A compact dual-band rectenna using slot-loaded dual band folded dipole antenna," *IEEE Antennas Wireless Propag. Lett.*, vol. 12, pp. 1634–1637, 2013.

[20] M. U. Rehman, W. Ahmad, and W. T. Khan, "Highly efficient dual band 2.45/5.85 GHz rectifier for RF energy harvesting applications in ISM band," in *Proc. Asia Pacific Microw. Conf.*, Nov. 2017, pp. 150–153.

[21] M. M. Mansour and H. Kanaya, "Compact RF rectifier circuit for ambient energy harvesting," in *Proc. IEEE Int. Symp. Radio-Freq. Integr. Technol. (RFIT)*, Aug./Sep. 2017, pp. 220–222.

[22] A. Collado and A. Georgiadis, "Conformal hybrid solar and electromagnetic (EM) energy harvesting rectenna," *IEEE Trans. Circuits Syst. I: Reg. Papers*, vol. 60, no. 8, pp. 2225–2234, Aug. 2013.

Aline Eid received the B.E. degree in electrical engineering from Notre Dame University—Louaize, Zouk Mosbeh, Lebanon, in 2015, and the master's degree in electromagnetics, antennas and RF systems from the American University of Beirut, Beirut, Lebanon, in 2017. She is currently pursuing the Ph.D. degree in electrical engineering with the Georgia Institute of Technology, Atlanta, GA, USA.

Her research interest focuses on the simulation, design, and fabrication of printed RF and millimeter-wave electronics, more specifically RF energy harvesting systems and fully printed active devices for reconfigurable systems.

Jimmy G. D. Hester received the M.S. and Ph.D. degrees in electrical and computer engineering from the Georgia Institute of Technology, Atlanta, GA, USA, in 2014 and 2019, respectively.

He is currently a Co-Founder of Atheraxon, Atlanta, the company commercializing the 5G RFID technology. He has been developing solutions for the use of carbon nanomaterials as well as optimized RF structures toward the implementation of inkjet-printed flexible low-cost ubiquitous gas sensors for the Internet of Things and smart skin applications. His work covers the entire development process, from the development of inkjet inks, improvement of fabrication methods, sensor component design, high-frequency characterization and environmental testing to the design, simulation, and fabrication of the RF system embedding the sensor, and the development of wireless reading and data processing schemes. His research interests lie at the interface between radio frequency and millimeter-wave engineering and material science, in the form of flexible electronics technologies and nanotechnologies.

Dr. Hester was awarded the 2015 NT4D Student Award, the 2nd Place Best Poster Award at the 2017 IEEE Futurecar Conference, the 3rd Place Best Poster Award at the 2017 Flex Conference, and the Honorable Mention Award as finalist of the 2017 IMS Student Paper Competition.

Joseph Costantine (SM'19) received the bachelor's degree from the Second Branch of the Faculty of Engineering, Lebanese University, Beirut, Lebanon, in 2004, the master's (M.E.) degree from the American University of Beirut, Beirut, in 2006, and the Ph.D. degree from The University of New Mexico, Albuquerque, NM, USA, in 2009.

He is currently an Associate Professor with the Electrical and Computer Engineering Department, American University of Beirut. He holds seven provisional and full U.S. patents. He has authored so far 2 books, 1 book chapter, and more than 150 journals and conference papers. His research interests reside in reconfigurable antennas for wireless communications, cognitive radio, RF systems for wireless energy harvesting, antennas and rectennas for the Internet of Things (IoT) devices, RF systems for biomedical devices, wireless characterization of dielectric material, and deployable antennas for small satellites.

Dr. Costantine received many awards and honors throughout his career including the 2008 IEEE Albuquerque Chapter Outstanding Graduate Award, the Three Year (2011–2013) Air Force Summer Faculty Fellowship with Kirtland's Space Vehicles Directorate in NM, USA, the 2017 First Prize at the Idea-Thon of International Healthcare Industry Forum, the 2018 Science and Technology Innovation Award, and the 2019 Excellence in Teaching Award from the American University of Beirut, in addition to several best paper awards and honorable mentions. He has been an Associate Editor of IEEE ANTENNAS AND WIRELESS PROPAGATION LETTERS since July 2018.

Youssef Tawk received the B.E. degree (with highest distinction) from Notre Dame University—Louaize, Zouk Mosbeh, Lebanon, in 2006, the M.E. degree from the American University of Beirut, Beirut, Lebanon, in 2007, and the Ph.D. degree from The University of New Mexico, Albuquerque, NM, USA, in 2011.

He served as a Valedictorian of his graduating class with Notre Dame University—Louaize. He is currently an Assistant Professor with the Electrical and Computer Engineering (ECE) Department, American University of Beirut. He has authored more than 140 IEEE journals and conference papers many of which received finalist positions and honorable mentions in several paper contests. He has coauthored two books and one book chapter, and holds seven U.S. patents. His research interests include reconfigurable RF systems for microwave and millimeter-wave applications, cognitive radio, optically controlled RF components, phased arrays, and phase shifters based on smart RF materials.

Dr. Tawk received many awards and honors such as the 2018 and 2014 Science and Technology Innovation Awards for his patents on reconfigurable microwave filters and optically controlled antenna systems and the 2011 IEEE Albuquerque Chapter Outstanding Graduate Award. He is an Associate Editor of the *Wiley Microwave and Optical Technology Letters*.

Ali H. Ramadan received the Ph.D. degree in electrical and computer engineering from the American University of Beirut, Beirut, Lebanon, in 2014.

In 2010, he joined the Cognitive Radio Research Group, Electrical and Computer Engineering Department, The University of New Mexico, Albuquerque, NM, USA, where he was a Ph.D. Exchange Research Scholar from 2010 to 2013. In 2014, he joined the Electrical and Computer Engineering Department, American University of Beirut, as a Post-Doctoral Fellow, where he held an associate research position, in 2017. He is currently an Assistant Professor with the Electrical Engineering Department, Fahad Bin Sultan University, Tabuk, Saudi Arabia. His current research interests include wireless power transfer, bioelectromagnetics, reconfigurable RF front-end transceivers for the Internet of Things (IoT) applications, and phased antenna arrays.

Manos M. Tentzeris (S'89–M'92–SM'03–F'10) received the Diploma degree *(magna cum laude)* in electrical and computer engineering from the National Technical University of Athens, Athens, Greece, in 1992, and the M.S. and Ph.D. degrees in electrical engineering and computer science from the University of Michigan, Ann Arbor, MI, USA, in 1994 and 1998, respectively.

He was a Visiting Professor with the Technical University of Munich, Munich, Germany, in 2002, with GTRI-Ireland, Athlone, Ireland, in 2009, and with LAAS-CNRS, Toulouse, France, in 2010. He is currently the Ken Byers Professor of flexible electronics with the School of Electrical and Computer Engineering, Georgia Institute of Technology, Atlanta, GA, USA, where he heads the ATHENA Research Group (20 researchers). He has served as the Head of the GTECE Electromagnetics Technical Interest Group, as the Georgia Electronic Design Center Associate Director of RFID/Sensors Research, as the Georgia Institute of Technology NSF-Packaging Research Center Associate Director of RF Research, and as the RF Alliance Leader. He has helped develop academic programs in 3-D/inkjet-printed RF electronics and modules, flexible electronics, origami and morphing electromagnetics, highly integrated/multilayer packaging for RF and wireless applications using ceramic and organic flexible materials, paper-based RFID's and sensors, wireless sensors and biosensors, wearable electronics, "Green" electronics, energy harvesting and wireless power transfer, nanotechnology applications in RF, microwave MEMS, and system on package (SOP)-integrated (UWB, multiband, mmW, and conformal) antennas. He has authored more than 650 articles in refereed journals and conference proceedings, 5 books, and 25 book chapters.

Dr. Tentzeris was a recipient/co-recipient of the 2019 Humboldt Research Prize, the 2017 Georgia Institute of Technology Outstanding Achievement in Research Program Development Award, the 2016 Bell Labs Award Competition 3rd Prize, the 2015 *IET Microwaves, Antennas, and Propagation* Premium Award, the 2014 Georgia Institute of Technology ECE Distinguished Faculty Achievement Award, the 2014 IEEE RFID-TA Best Student Paper Award, the 2013 *IET Microwaves, Antennas and Propagation* Premium Award, the 2012 FiDiPro Award in Finland, the iCMG Architecture Award of Excellence, the 2010 IEEE Antennas and Propagation Society Piergiorgio L. E. Uslenghi Letters Prize Paper Award, the 2011 International Workshop on Structural Health Monitoring Best Student Paper Award, the 2010 Georgia Institute of Technology Senior Faculty Outstanding Undergraduate Research Mentor Award, the 2009 IEEE TRANSACTIONS ON COMPONENTS AND PACKAGING TECHNOLOGIES Best Paper Award, the 2009 E. T. S. Walton Award from the Irish Science Foundation, the 2007 IEEE AP-S Symposium Best Student Paper Award, the 2007 IEEE MTT-S IMS Third Best Student Paper Award, the 2007 ISAP 2007 Poster Presentation Award, the 2006 IEEE MTT-S Outstanding Young Engineer Award, the 2006 Asia–Pacific Microwave Conference Award, the 2004 IEEE TRANSACTIONS ON ADVANCED PACKAGING Commendable Paper Award, the 2003 NASA Godfrey "Art" Anzic Collaborative Distinguished Publication Award, the 2003 IBC International Educator of the Year Award, the 2003 IEEE CPMT Outstanding Young Engineer Award, the 2002 International Conference on Microwave and Millimeter-Wave Technology Best Paper Award (Beijing, China), the 2002 Georgia Institute of Technology—ECE Outstanding Junior Faculty Award, the 2001 ACES Conference Best Paper Award, the 2000 NSF CAREER Award, and the 1997 Best Paper Award of the International Hybrid Microelectronics and Packaging Society. He was the TPC Chair of the IEEE MTT-S IMS 2008 Symposium and the 2005 IEEE CEM-TD Workshop. He is the Vice-Chair of the RF Technical Committee (TC16) of the IEEE CPMT Society. He is the Founder and the Chair of the RFID Technical Committee (TC24) of the IEEE MTT-S and the Secretary/Treasurer of the IEEE C-RFID. He is an Associate Editor of the IEEE TRANSACTIONS ON MICROWAVE THEORY AND TECHNIQUES, the IEEE TRANSACTIONS ON ADVANCED PACKAGING, and the *International Journal on Antennas and Propagation*. He has given more than 100 invited talks to various universities and companies all over the world. He is a member of the URSI-Commission D and the MTT-15 Committee, an Associate Member of EuMA, a fellow of the Electromagnetic Academy, and a member of the Technical Chamber of Greece. He served as one of the IEEE MTT-S Distinguished Microwave Lecturers from 2010 to 2012 and is one of the IEEE CRFID Distinguished Lecturers.